NJC

Accepted Manuscript

ROYAL SOCIETY
OF CHEMISTRY

www.rsc.org/njc

New Journal of Chemistry RSCPublishing

ARTICLE

Fluorous-Inorganic Hybrid Dielectric Materials for Solution-Processed Electronic Devices

wwwCite this: DOI: 10.1039/x0xx00000x

Received 00th January 2012, Accepted 00th January 2012

DOI: 10.1039/x0xx00000x

www.rsc.org/

Heejin Kim,[a] Sang Ho Jo,[b] Joong-Hwi Ji,[a] WooJe Han,[c] Youngtae Kim,[a] Hyung-Ho Park,[c] Hyoung-Joon Jin,[a] Byungwook Yoo,*[b] and Jin-Kyun Lee*[a]

We report the synthesis and characterisation of fluorous-inorganic hybrid dielectric (FIHD) materials processable in highly fluorinated orthogonal solvents for printed electronic devices. FIHD materials were prepared successfully via ligand exchange reactions between organic ligands on the surfaces of nanomaterials and highly fluorinated carboxylic acids. When hafnium oxide (HfO_2) or zirconium oxide (ZrO_2) nanoparticles stabilized with trioctylphosphine oxide (TOPO) were treated with perfluoro-3,6,9-trioxatridecanoic acid in HFE-7500 at 130 °C, the modified surface characteristics of the nanoparticles resulted in excellent solubilities in the fluorous solvent. The dielectric constant of HfO_2 and ZrO_2 nanoparticles modified with the fluorous acid were *ca.* 4.4 and 4.3 at 1 KHz, respectively, which are significantly higher than those of fluoropolymers. Top-gate organic thin film transistors (OTFTs) were fabricated using solution-processed organic semiconductors and HfO_2-based FIHD materials. The hole mobilities of the OTFTs produced were as high as 0.08 cm^2/Vs (Vds = -40V) and the on/off ratio reached 3.3×10^6 when 2,8-difluoro-5,11-bis(triethylsilylethynyl)anthradithiophene (diF-TESADT) was employed in the semiconductor layer. These device performances demonstrate that FIHD materials can be useful components for general printed electronic devices processed with soluble organic electronic materials.

Introduction

High performance organic thin-film-transistors (OTFTs) have drawn a good deal of attention for their potential applications in flexible active-matrix displays, non-volatile memories and sensors, just to name a few.[1-5] In general, OTFTs are fabricated with metal electrodes, dielectric and organic semiconductor layers, and high capacitance gate dielectric materials play important roles in reducing driving voltages and improve the charge transfer characteristics of transistors.[6] Apart from their performances, dielectric materials also affect the way of producing OTFTs. If these materials are deposited by vacuum thermal evaporation or atomic layer deposition, the technical and cost issues arise when OTFTs are incorporated into affordable, large-area, flexible electronic products.[7, 8]

Numerous inorganic dielectric materials have been reported, such as, $BaTiO_3$,[9, 10] $SrTiO_3$,[11] ZrO_2,[12] HfO_2,[13] TiO_2,[14] Y_2O_3,[15]and Al_2O_3.[16] However, despite the remarkable progress made at increasing dielectric constant, these inorganic compounds have a critical disadvantage, as they cannot be applied by solution processing, which is one of the most promising techniques for future electronics fabrication. Polymeric materials have also been studied extensively because their films can be deposited conveniently by employing their solutions in organic or aqueous solvents. However, solution-processable polymeric materials are limited by relatively low dielectric constant.[17-20] In addition, the use of polymer solutions introduces chemical compatibility issues among organic materials, including processing solvents, when they are used to fabricate multi-layer organic devices. When one attempts to deposit a dielectric polymer solution onto a predefined organic semiconductor film (in the case of top gate OTFTs), physical and/or chemical damage occurs in the semiconductor layer, and this diminishes device performance.[21-29]

In order to resolve these issues, we undertook the development of insulating materials which have sufficiently high dielectric constant and processability in highly fluorinated (or fluorous) solvents, such as, hydrofluoroethers (one example shown in **Figure 1a**) and perfluorocarbons. Since the aforementioned solvents have a chemically benign nature and limited miscibility with a large number of organic materials, we considered a dielectric material solution in such solvents would not damage other functional organic films, especially the organic semiconductor layer.[30-34]

The concept of depositing non-damaging fluoropolymer solutions onto organic semiconductor films is not new.

Amorphous fluoropolymers, such as CYTOP^{TM} and TEFLON-AF^{TM}, have already been investigated for this purpose in their solution forms dissolved in perfluorocarbons.[35] Although these polymers are able to produce uniform coatings on organic semiconductors, their low dielectric constant, which are as low as 2, remain at issue.[36]

Then, how can sufficiently high dielectric constant and processability in fluorous solvents be achieved simultaneously? To answer this question, we considered inorganic nanomaterials with surfaces modified by fluorinated ligands.[37, 38] It has been well established that the solubility or dispersible character of nanomaterials in solvents can be determined by their surface modifiers.[39] For example, oleic acids or trioctylphosphine oxide (TOPO) ligands make nanomaterials soluble in organic solvents, such as hexanes. Thus, we sought to develop *fluorous-inorganic hybrid dielectric (FIHD)* materials by modifying the surfaces of inorganic nanoparticles with highly fluorinated molecules containing surface-adhering functional groups.

In this study, two model dielectric materials, hafnium oxide (**1**, HfO_2, k = 25 in bulk) and zirconium oxide (**2**, ZrO_2, k = 25 in bulk)[40, 41] nanoparticles were prepared with TOPO ligands. Subsequent ligand exchange reactions were used to introduce fluorous carboxylic acid ligands on their surfaces (**Figure 1c**), which allowed these nanoparticles to dissolve in fluorous solvents. Furthermore, solutions of these FIHD materials exhibited excellent coating properties on solution-processed organic semiconductors and the OTFTs produced showed promising performances.

Experimental

Materials

Hafnium(IV) chloride (99.9%), hafnium(IV) isopropoxide isopropanol adduct (99%) and perfluorooctadecanoic acid (97%) were purchased from Alfa Aesar, UK and used as received. Zirconium(IV) chloride (99.9%) and zirconium(IV) isopropoxide isopropanol adduct (99%) were obtained from Sigma-Aldrich and used without further purification. Tri-*n*-octylphosphineoxide (99%) and perfluoro-3,6,9-trioxatridecanoic acid (98%) were purchased from Acros and Fluorochem, UK, respectively. Nonadecafluorodecanoic acid was obtained from TCI and used as received. Fluorous solvents, such as, HFE-7500, were obtained from 3M, Korea.

Preparations of HfO_2 (1) and ZrO_2 (2) nanoparticles

HfO_2 nanoparticles were synthesized as described by Jing Tang, *et al* (**Figure S1a**).[42] Briefly, hafnium(IV) isopropoxide isopropanol adduct (0.95 g, 2 mmol) and hafnium(IV) chloride (0.65 g, 2 mmol) were added to a flask containing TOPO (10.0 g, 26 mmol) under a N_2 atmosphere. The reaction mixture was heated quickly to 360 °C and held at that temperature for 2 h with vigorous stirring. The reaction vessel was then cooled to 60 °C and a large volume of acetone was added to precipitate HfO_2 nanoparticles. The solid was collected by centrifugation and washed with acetone several times. The HfO_2 nanoparticles stabilised with TOPO were then re-dispersed in hexanes (20 cm^3) and the resulting solution was filtered through a syringe filter (PTFE, pore size 0.45 micron). Purified HfO_2 nanoparticles were reprecipitated by pouring acetone (40 cm^3) into the filtered hexanes solution to give HfO_2 nanoparticles (0.5 g).

ZrO_2 nanoparticles were also successfully produced as described by Jin Joo, *et al* (**Figure S1b**), using a procedure similar to that described above.[43]

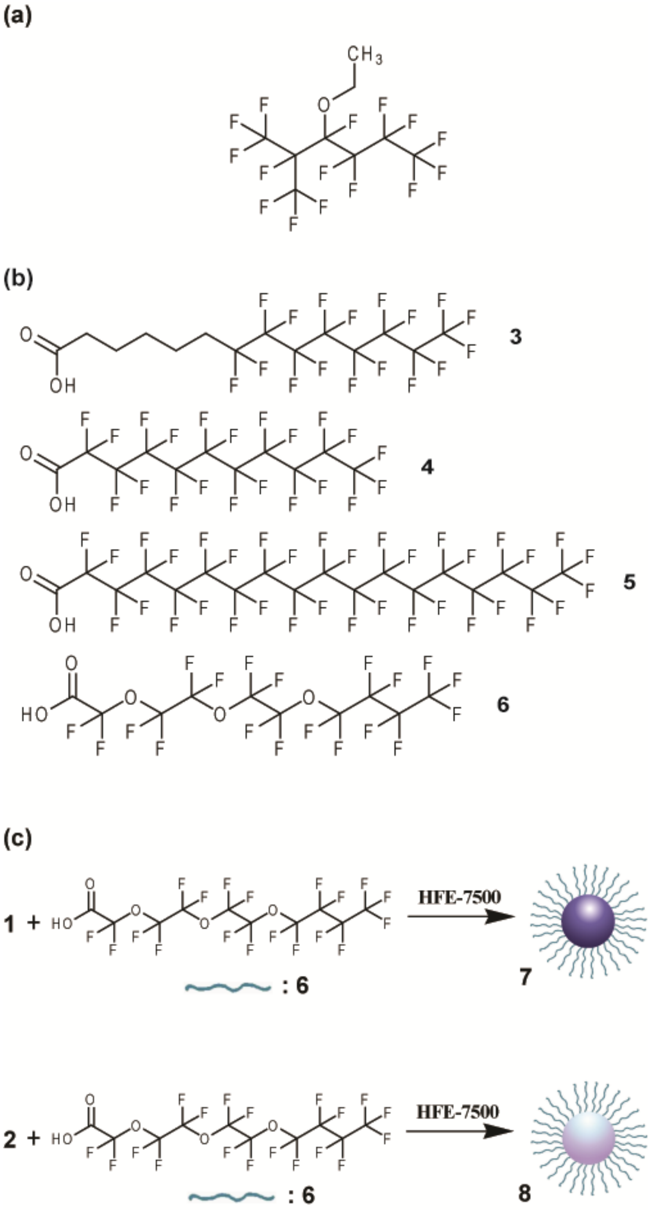

Figure 1. Chemical structures of (a) HFE-7500 and (b) fluorous ligands employed in the ligand exchange experiments. (c) Ligand exchange reactions with HfO_2 (**1**) and ZrO_2 (**2**).

Ligand Exchange of TOPO-capped HfO_2 and ZrO_2 nanoparticles with highly fluorinated carboxylic acids

HfO_2 nanoparticles (or ZrO_2, 0.5 g) and perfluoro-3,6,9-trioxatridecanoic acid (**6**, **Figure 1b**, 1.5 g) were added to a flask containing HFE-7500 (5 cm^3). After stirring for 5 h at 130 °C, the solution was cooled to room temperature. An excess of acetone was then added to the mixture to precipitate the ligand-substituted nanoparticles. The resulting solid was collected by centrifugation and dried under reduced pressure to give the FIHD material **7** (0.7 g).

Characterisations of hybrid dielectric materials

Transmission electron microscope (TEM) experiments were conducted using a Philips CM200 unit at accelerating voltage of 200 kV. A Zeta potential analyzer (ELS-Z) was used to confirm the particle size distribution of nanomaterials in HFE-7500. Infrared spectra of nanoparticles were obtained using a Bruker VERTEX 80V at a resolution of 4 cm^{-1}. Samples were prepared by pelletizing with KBr. Thermogravimetric analysis (TGA) was performed on a STA409PC at a heating rate of 10 °C/min in a N_2 atmosphere. X-Ray diffraction (XRD) measurements were carried out using a Rigaku Ultima IV and CuKa radiation. To obtain nanoparticles suitable for X-ray diffraction (XRD) experiments, a drop of HfO_2 or ZrO_2 solution was placed on a Si substrate and the solvent was allowed to evaporate.

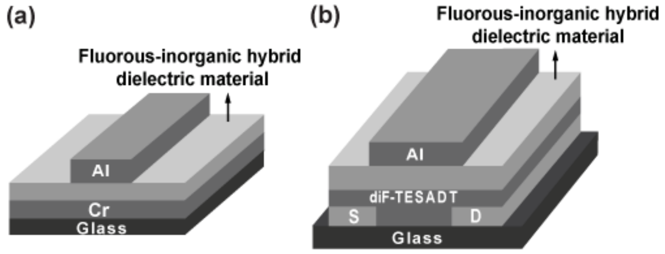

Figure 2. Device configurations of (a) MIM-type diode and (b) top-gate OTFT.

Fabrication and characterisation of devices

In order to evaluate the dielectric properties of FIHD materials, metal-insulator-metal (MIM) diodes were fabricated as shown in **Figure 2a**. Cr-coated glass was used as a substrate, which was cleaned by sequential sonication in acetone, methanol, and isopropanol for 5 min each. After dissolving a FIHM material in HFE-7500 [concentration, 10% (wt/vol)], the resulting solution was spin-coated on a Cr-coated glass plate at 1,500 rpm for 1 min. The substrate was then baked at 70 °C for 30 min and annealed further at 100 °C for 30 min to remove residual solvents. Thin film thicknesses were measured using a KLA-Tencor step profiler. The thicknesses of ligand substituted HfO_2 and ZrO_2 films were 180 nm and 260 nm, respectively. A top Al electrode (thickness 100 nm) was thermally evaporated onto the FIHD layer through a shadow mask, which completed the fabrication of MIM diodes for dielectric constant measurements.

Organic thin film transistors (OTFTs) were also fabricated in the top-gate configuration (**Figure 2b**). Au source and drain electrodes (thickness 100 nm) were deposited on a glass substrate covered with a 2.5 nm-thick Cr adhesion layer by vacuum thermal evaporation. A solution of p-type organic semiconductor, [2,8-difluoro-5,11-bis(triethylsilylethynyl)anthradithiophene (diF-TESADT)], in chlorobenzene [concentration: 1% (wt/vol)] was spin-coated at 1,000 rpm for 20 s. After annealing the organic semiconductor film at 100 °C for 30 min, a FIHD material solution in HFE-7500 was spin-coated on top of the semiconductor layer at 1,500 rpm for 1 min. The resulting FIHD film was baked at 70 °C for 30 min and annealed further at 150 °C for 30 min. Finally, an Al gate electrode (thickness 100 nm) was thermally deposited on the FIHD layer.

Results and discussion

In order to develop FIHD materials, we started from the syntheses of HfO_2 (**1**) and ZrO_2 (**2**) nanoparticles stabilised with TOPO using a non-hydrolytic sol-gel method.[42, 43] Because the metal oxide nanoparticles obtained were stabilised by an organic ligand, they were soluble in organic solvents, in particular, in non-polar hydrocarbons. TEM images showed that the sizes and shapes of both nanoparticles were uniform. HfO_2 nanoparticles were rod shaped and about 13×3 nm (**Figure S2a** in Supporting Info.), and ZrO_2 nanoparticles were spherical with diameters of *ca*. 3 nm (**Figure S2d** in Supporting Information). High-resolution TEM images of nanoparticles revealed that the growth lattice plane of HfO_2 was {001} and that of ZrO_2 was {011} (**Figures S2b**, **c**, **e** and **f** in Supporting Information). X-ray diffraction patterns confirmed the crystalline structures of both metal oxide nanoparticles. Inside the nanostructure, HfO_2 crystallized in the monoclinic phase, whereas ZrO_2 crystallized in the tetragonal phase (**Figure S3** in Supporting Information).[44] The reference patterns of the monoclinic phase (JCPDS 34-0104) of HfO_2 and the tetragonal phase (JCPDS 50-1089) of ZrO_2 are shown in **Figure S3** in Supporting Information.

Following the successful synthesis of HfO_2 and ZrO_2 nanomaterials, ligand exchange reactions were carried out to substitute surface TOPO ligands with fluorous ligands (**Figure 1c**). The purified TOPO-stabilized nanoparticles were reacted with various fluorous carboxylic acids in HFE-7500 at 130 °C. The chemical structures of employed acids are shown in **Figure 1b**. Here, the acid **3**, synthesized from diethyl malonate and a semi-perfluorododecyl iodide (Supporting Information), was considered at first because we expected it could be introduced onto the oxide surface in a similar fashion to the conventional oleic acid ligand. The acids **4** and **5** were also included because of their greater acid strengths than acid **3**, which we considered would increase the strengths of binding interactions with basic metal oxides. Because the perfluoroalkyl chain of the acid **5** is longer than that of the acid **4**, better solubilizing ability was expected for acid **5** in HFE-7500. Along with carboxylic acids possessing stiff perfluoroalkyl chains, perfluoro-3,6,9-trioxatridecanoic acid (**6**), which has perfluoroether linkages, was also investigated.

During exchange reactions spanning 5 h, chunky agglomerates of HfO_2 and ZrO_2 in HFE-7500 disappeared gradually in the presence of fluorous carboxylic acids, resulting in the formation of pale-green transparent solutions (**Figure 3a**). On the other hand, the TOPO-stabilised agglomerates in the absence of acid, showed no evidence of dissolution in the same solvent. Of the acids presented in **Figure 1b**, acid **6** was found to have the most promising solubilizing capabilities. This is believed to be due to the flexible nature of the perfluoroether linkages, which enabled the acid **6** to interact more favourably with solvent molecules. Along with short-term observations, long-term storage tests were performed with FIHD materials treated with acid **6**, and no precipitation of metal oxide particles was detected on the bottoms of the vials after 6 months. These results convinced us that the fluorous solutions have high enough dispersion stabilities to cast thin films of FIHD materials.

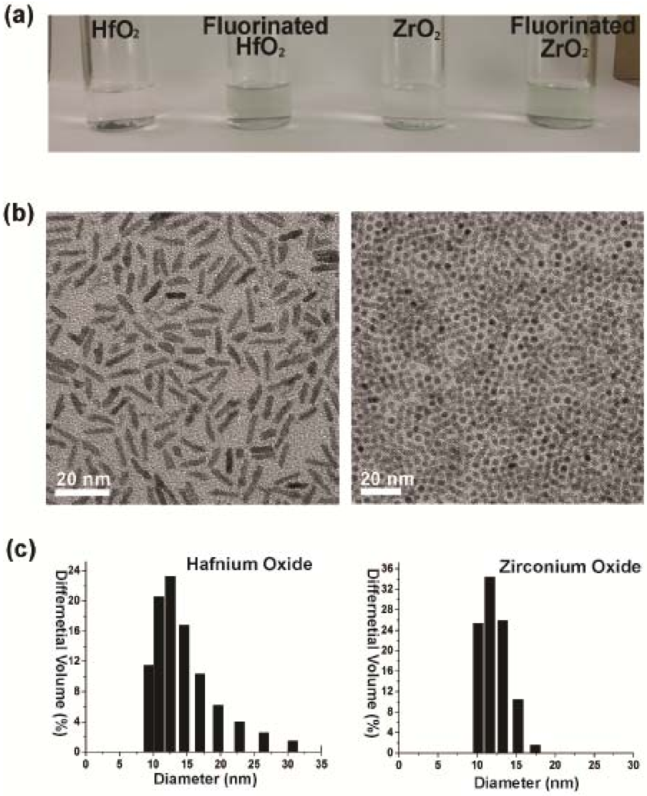

Figure 3. (a) Pictures of TOPO-stabilised metal oxide nanoparticles and fluorous ligand-substituted nanoparticles in HFE-7500, (b) low-magnification TEM images of HfO_2 nanorods and ZrO_2 nanospheres treated with fluorous acids on a carbon-coated copper grid, (c) particle size analysis data of fluorous acid-substituted HfO_2 and ZrO_2 in HFE-7500.

Together with visual observations, we studied the characteristics of metal oxide solutions by TEM and by using a particle size analyser. TEM images of HfO_2 and ZrO_2 nanoparticles (**Figure 3b**) indicated that the fluorous acid-treated particles did not aggregate compared to their states before ligand exchange (**Figure S2** in Supporting Information). Particle size analysis in HFE-7500 (**Figure 3c**) also showed hardly any changes in the size distribution of nanoparticles occurred during ligand exchange. The HfO_2 existed evenly dispersed in HFE-7500 with a particle size distribution in between 9 to 30 nm, whereas the particle size distribution ZrO_2 was from 10 to 17 nm.

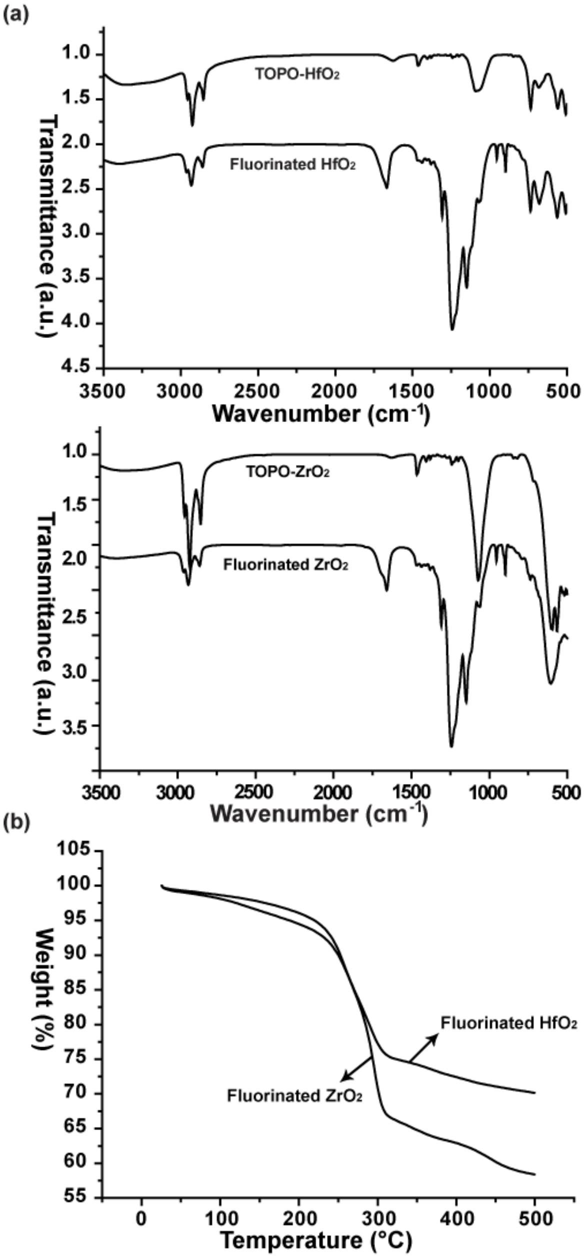

Figure 4. (a) FT-IR spectra of TOPO-stabilised HfO_2 (**1**)/ZrO_2 (**2**) and fluorous ligand-modified HfO_2 (**7**)/ZrO_2 (**8**) particles, (b) Thermogravimetric analysis of fluorous ligand-modified HfO_2 (**7**) and ZrO_2 (**8**) particles.

In addition, we investigated chemical changes on nanoparticle surfaces during the course of ligand substitution by FT-IR spectroscopy (**Figure 4a**). When we examined the spectra of HfO_2 (**1**) and ZrO_2 (**2**), the absorption bands at approximately 1,070 – 1,090 cm^{-1} of the P=O stretching in TOPO ligands were clearly visible.[45, 46] On the other hand, strong absorption peaks between 1,000 and 1,500 cm^{-1} of the fluorous ligand-modified nanoparticles appeared, which could be interpreted by the presence of perfluoro-3,6,9-trioxatridecanoic acid on the metal oxide surface.[47, 48] Along with the peaks resulting from perfluoroether moieties, fluorous ligand-modified HfO_2 (**7**) and ZrO_2 (**8**) exhibited absorption peaks at *ca.* 1,670 cm^{-1}, indicating the presence of carbonyl groups introduced by the carboxylic acid.[49]

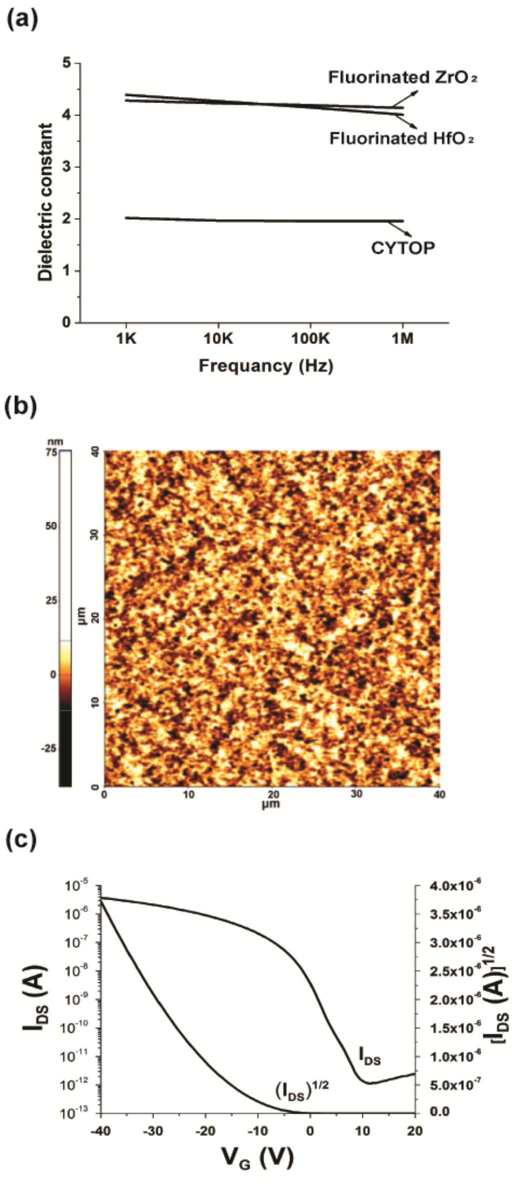

Figure 5. (a) Dielectric constant of FIHD material films at frequencies from 1 KHz to 1 MHz at room temperature, (b) 40 *µm* x 40 *µm* AFM image of the FIHD HfO_2 film, (c) charge transfer characteristics of a diF-TESADT-based transistor using FIHD HfO_2 as a gate dielectric layer (devices had a channel width of 900 µm and a channel length of 85 µm. The operating source-drain voltage was -40 V).

The thermal behaviours of FIHD materials were also investigated to obtain more information on the ligand exchange reactions. When we examined the TGA plots of TOPO-stabilised nanoparticles (**1** and **2**) (**Figure S4** in Supporting Information), we found that weights of TOPO-stabilised nanoparticles decreased by 9% and 18% at 500 °C for HfO_2 and ZrO_2, respectively. These weight losses indicated the dissociation of TOPO. On the other hand, the weight losses of fluorous ligand-modified nanoparticles were 30% and 42% for HfO_2 and ZrO_2, respectively, as shown in **Figure 4b**. These larger changes in weights demonstrate that a considerable number of TOPO molecules were substituted with fluorous carboxylic acids, as these are substantially heavier but more volatile than TOPO molecules.

Finally, we evaluated the electrical properties of the FIHD materials, including their dielectric constant and charge transfer characteristics. Typical metal-insulator-metal (MIM) diodes were fabricated to examine their dielectric characteristics (**Figure 2a**). Along with the FIHD materials, CYTOP™ (a well-known commercially available fluoropolymer) was chosen as a reference. **Figure 5a** summarizes dielectric constant measurements, and shows that values for fluorous ligand-modified HfO_2 (**7**) and ZrO_2 (**8**) were *ca.* 4.4 and 4.3 at 1 kHz frequency, respectively. On the other hand, the dielectric constant for CYTOP™ was 2.0. At higher frequencies, the dielectric constant of the FIHD materials were still two times higher than that of CYTOP.

To get a step closer to the actual application of FIHD materials, the surface morphologies of the HfO_2 nanoparticle-based gate dielectric film were examined. **Figure 5b** shows a 40 *µm* x 40 *µm* atomic force microscopic (AFM) image of the film. The root mean square (RMS) roughness of the film was 6.0 nm.

Motivated by the dielectric constant measurements and the surface analysis, we manufactured OTFTs employing a FIHD layer, as shown in **Figure 2b** (The channel width and channel length of the device were 900 µm and 85 µm, respectively). The strong benefit of using fluorous solvent-soluble materials lies in their processabilities, such as, their ability to be directly cast onto fragile organic semiconductor films. **Figure 5c** shows the charge transfer characteristic of a top-gate diF-TESADT transistor operating at a source-drain voltage of -40 V. Electrical measurements performed under ambient air conditions at room temperature showed that the organic semiconductor layer was not damaged during the casting of FIHD materials from solution. The field-effect mobility calculated in the saturation regime was 0.08 $cm^2 V^{-1} s^{-1}$, and a threshold voltage of 4.67 V was obtained at a source-drain voltage of -40 V. The on/off current ratio was 3.3×10^6. The device performance was comparable to that of previously reported device fabricated with CYTOP™ as a gate dielectric material.[50, 51] These successful results indicate that the proposed dielectric materials developed on the fluorous-inorganic hybrid concept are suitable for real applications, particularly in the display backplanes, thanks to their processability and performance advantages.

Conclusions

In this study, we introduce the concept of fluorous-inorganic hybrid dielectric (FIHD) materials processable with highly fluorinated solvents. FIHD materials were prepared successfully using ligand substitution reactions between nanoparticle surface bound trioctylphosphine oxide (TOPO) and highly fluorinated carboxylic acids, in particular, perfluoro-3,6,9-trioxatridecanoic acid (**6**). The nanoparticles produced showed excellent solubilities in HFE-7500. The dielectric constant of the fluorous acid-modified HfO_2 and ZrO_2 nanoparticles were *ca*. 4.4 and 4.3 at 1 KHz, respectively, which are significantly higher than those of fluoropolymers, such as, CYTOP^{TM}. To demonstrate the concept, top-gate organic thin film transistors were fabricated using a solution-processed organic semiconductor layer and the HfO_2-based FIHD material. The mobility of an thin-film-transistor (OTFT) was 0.08 cm^2 V^{-1} s^{-1} (V_{ds} = -40 V) and the on/off ratio reached 3.3×10^6 when 2,8-difluoro-5,11-bis(triethylsilylethynyl) anthradithiophene (diF-TESADT) was used as an organic semiconductor layer. This device performance indicates that FIHD materials could be useful components for general printed electronic devices processed with soluble organic electronic materials.

Acknowledgements

This study was supported by a grant (#10041220) from the Fundamental R&D Program for Core Technology of Materials funded by the Ministry of Trade, Industry & Energy, Republic of Korea. J.K.L thanks Inha University for partial support.

Notes and references

[a]Department of Polymer Science and Engineering, Inha University, Incheon 402-751, South Korea.

[b]Korea Electronics Technology Institute, Seongnam-si, Gyeonggi-do, 463-816, South Korea.

[c]Department of Materials Science and Engineering, Yonsei University, Seoul 120-749, South Korea.
Fax: +82328655178; E-mail: jkl36@inha.ac.kr (J.-K. Lee)
E-mail: bwyoo@keti.re.kr (B. Yoo)

† The first three authors contributed equally to this work. Electronic Supplementary Information (ESI) available: synthesis of a semi-perfluorinated acid, TEM images and thermal analysis data. See DOI: 10.1039/b000000x/

1. S. Lee, B. Koo, J. G. Park, H. Moon, J. Hahn and J. M. Kim, *MRS Bull.*, 2006, **31**, 455-459.
2. C. D. Dimitrakopoulos and P. R. L. Malenfant, *Adv Mater*, 2002, **14**, 99-+.
3. H. Yan, Z. H. Chen, Y. Zheng, C. Newman, J. R. Quinn, F. Dotz, M. Kastler and A. Facchetti, *Nature*, 2009, **457**, 679-U671.
4. G. Horowitz, *J. Mater. Res.*, 2004, **19**, 1946-1962.
5. L. Jiang, J. Zhang, D. Gamota and C. G. Takoudis, *Org. Electron.*, 2010, **11**, 959-963.
6. S. A. DiBenedetto, A. Facchetti, M. A. Ratner and T. J. Marks, *Adv Mater*, 2009, **21**, 1407-1433.
7. J. Li, D. Liu, Q. Miao and F. Yan, *J. Mater. Chem.*, 2012, **22**, 15998-16004.
8. Y. G. Ha, S. Jeong, J. S. Wu, M. G. Kim, V. P. Dravid, A. Facchetti and T. J. Marks, *J. Am. Chem. Soc.*, 2010, **132**, 17426-17434.
9. Z. Zhao, V. Buscaglia, M. Viviani, M. T. Buscaglia, L. Mitoseriu, A. Testino, M. Nygren, M. Johnsson and P. Nanni, *Phys Rev B*, 2004, **70**.
10. P. Firek, A. Werbowy and J. Szmidt, *Materials Science and Engineering B-Advanced Functional Solid-State Materials*, 2009, **165**, 126-128.
11. G. A. Seisenbaeva, S. Gohil, V. G. Kessler, M. Andrieux, C. Legros, P. Ribot, M. Brunet and E. Scheid, *Appl. Surf. Sci.*, 2011, **257**, 2281-2290.
12. W.-J. Qi, R. Nieh, B. H. Lee, L. Kang, Y. Jeon and J. C. Lee, *Appl. Phys. Lett.*, 2000, **77**, 3269-3271.
13. Y. S. Lin, R. Puthenkovilakam and J. P. Chang, *Appl. Phys. Lett.*, 2002, **81**, 2041-2043.
14. M. Kadoshima, M. Hiratani, Y. Shimamoto, K. Torii, H. Miki, S. Kimura and T. Nabatame, *Thin Solid Films*, 2003, **424**, 224-228.
15. J. S. Lee, W. H. Kim, I. K. Oh, M. K. Kim, G. Lee, C. W. Lee, J. Park, C. Lansalot-Matras, W. Noh and H. Kim, *Appl. Surf. Sci.*, 2014, **297**, 16-21.
16. S. Kim, J. Nah, I. Jo, D. Shahrjerdi, L. Colombo, Z. Yao, E. Tutuc and S. K. Banerjee, *Appl. Phys. Lett.*, 2009, **94**.
17. H. Klauk, M. Halik, U. Zschieschang, G. Schmid, W. Radlik and W. Weber, *J. Appl. Phys.*, 2002, **92**, 5259-5263.
18. T. H. Huang, H. C. Huang and Z. W. Pei, *Org. Electron.*, 2010, **11**, 618-625.
19. C. Wang, W.-Y. Lee, R. Nakajima, J. Mei, D. H. Kim and Z. Bao, *Chem. Mater.*, 2013, **25**, 4806-4812.
20. J. S. Meena, M.-C. Chu, Y.-C. Chang, C.-S. Wu, C.-C. Cheng, F.-C. Chang and F.-H. Ko, *ACS Applied Materials & Interfaces*, 2012, **4**, 3261-3269.
21. T. W. Lee, J. H. Shin, I. N. Kang and S. Y. Lee, *Adv Mater*, 2007, **19**, 2702-+.
22. C. D. Dimitrakopoulos, S. Purushothaman, J. Kymissis, A. Callegari and J. M. Shaw, *Science*, 1999, **283**, 822-824.
23. A. Javey, H. Kim, M. Brink, Q. Wang, A. Ural, J. Guo, P. McIntyre, P. McEuen, M. Lundstrom and H. J. Dai, *Nat Mater*, 2002, **1**, 241-246.
24. H. Sirringhaus, *Adv Mater*, 2005, **17**, 2411-2425.
25. Q. J. Cai, Y. Gan, M. B. Chan-Park, H. B. Yang, Z. S. Lu, C. M. Li, J. Guo and Z. L. Dong, *Chem. Mater.*, 2009, **21**, 3153-3161.
26. R. P. Ortiz, A. Facchetti and T. J. Marks, *Chem. Rev.*, 2010, **110**, 205-239.
27. C. G. Lee and A. Dodabalapur, *J. Electron. Mater.*, 2012, **41**, 895-898.
28. Y. Zhou, S. T. Han, Z. X. Xu, X. B. Yang, H. P. Ng, L. B. Huang and V. A. L. Roy, *J. Mater. Chem.*, 2012, **22**, 14246-14253.
29. B. Sun, W. Hong, Z. Yan, H. Aziz and Y. Li, *Adv Mater*, 2014, DOI: 10.1002/adma.201305981, n/a-n/a.
30. J.-K. Lee, H. H. Fong, A. A. Zakhidov, G. E. McCluskey, P. G. Taylor, M. e. Santiago-Berrios, H. D. Abruna, A. B. Holmes, G. G. Malliaras and C. K. Ober, *Macromolecules*, 2010, **43**, 1195-1198.
31. H. H. Fong, J. K. Lee, Y. F. Lim, A. A. Zakhidov, W. W. Wong, A. B. Holmes, C. K. Ober and G. G. Malliaras, *Adv Mater*, 2011, **23**, 735-739.

32. A. A. Zakhidov, J. K. Lee, J. A. DeFranco, H. H. Fong, P. G. Taylor, M. Chatzichristidi, C. K. Ober and G. G. Malliaras, *Chem Sci*, 2011, **2**, 1178-1182.
33. A. A. Zakhidov, J.-K. Lee, H. H. Fong, J. A. DeFranco, M. Chatzichristidi, P. G. Taylor, C. K. Ober and G. G. Malliaras, *Adv Mater*, 2008, **20**, 3481-3484.
34. J.-K. Lee, M. Chatzichristidi, A. A. Zakhidov, P. G. Taylor, J. A. DeFranco, H. S. Hwang, H. H. Fong, A. B. Holmes, G. G. Malliaras and C. K. Ober, *J. Am. Chem. Soc.*, 2008, **130**, 11564-11565.
35. T. Umeda, D. Kumaki and S. Tokito, *Org. Electron.*, 2008, **9**, 545-549.
36. J. Veres, S. Ogier, G. Lloyd and D. De Leeuw, *Chem. Mater.*, 2004, **16**, 4543-4555.
37. X. Zhang, H. Chen, Y. Ma, C. Zhao and W. Yang, *Appl. Surf. Sci.*, 2013, **277**, 121-127.
38. K. Yang, X. Huang, Y. Huang, L. Xie and P. Jiang, *Chem. Mater.*, 2013, **25**, 2327-2338.
39. S. Kango, S. Kalia, A. Celli, J. Njuguna, Y. Habibi and R. Kumar, *Prog. Polym. Sci.*, 2013, **38**, 1232-1261.
40. J. Robertson, *Eur Phys J-Appl Phys*, 2004, **28**, 265-291.
41. J. Robertson, *Rep. Prog. Phys.*, 2006, **69**, 327-396.
42. J. Tang, J. Fabbri, R. D. Robinson, Y. M. Zhu, I. P. Herman, M. L. Steigerwald and L. E. Brus, *Chem. Mater.*, 2004, **16**, 1336-1342.
43. J. Joo, T. Yu, Y. W. Kim, H. M. Park, F. X. Wu, J. Z. Zhang and T. Hyeon, *J. Am. Chem. Soc.*, 2003, **125**, 6553-6557.
44. X. Y. Zhao and D. Vanderbilt, *Phys Rev B*, 2002, **65**.
45. H. Li, C. Han and L. Zhang, *J. Mater. Chem.*, 2008, **18**, 4543-4548.
46. K. Faghihi and K. Zamani, *J. Appl. Polym. Sci.*, 2006, **101**, 4263-4269.
47. R. E. Moynihan, *J. Am. Chem. Soc.*, 1959, **81**, 1045-1050.
48. R. Buzzoni, S. Bordiga, G. Ricchiardi, G. Spoto and A. Zecchina, *The Journal of Physical Chemistry*, 1995, **99**, 11937-11951.
49. S. E. Cabaniss, *Anal. Chim. Acta*, 1991, **255**, 23-30.
50. N. Shin, J. Kang, L. J. Richter, V. M. Prabhu, R. J. Kline, D. A. Fischer, D. M. DeLongchamp, M. F. Toney, S. K. Satija, D. J. Gundlach, B. Purushothaman, J. E. Anthony and D. Y. Yoon, *Adv. Funct. Mater.*, 2013, **23**, 366-376.
51. J. Smith, R. Hamilton, Y. Qi, A. Kahn, D. D. C. Bradley, M. Heeney, I. McCulloch and T. D. Anthopoulos, *Adv. Funct. Mater.*, 2010, **20**, 2330-2337.